

Enhanced Intersystem Crossing in Gable-Type Copper(II) Porphyrin–Free Base Porphyrin Dimers: Evidence of Through-Bond Exchange Interaction

Namiki Toyama, Motoko Asano-Someda,* Takatoshi Ichino,† and Youkoh Kaizu

Department of Chemistry, Tokyo Institute of Technology, O-okayama, Meguro-ku, Tokyo, 152-8551, Japan

Received: November 29, 1999; In Final Form: March 9, 2000

Spacer dependence of intersystem crossing (ISC) affected by a remote metal unpaired electron was studied in a series of copper(II) porphyrin–free base porphyrin dimers. In these dimers, fluorescence of the free base moiety is remarkably quenched by the copper counterpart which is linked via a phenanthrene, a naphthalene, or a benzene. Fluorescence lifetimes and quantum yields of the free base moiety in the heterodimers are 1/10–1/35 of the free base monomer depending upon the spacer, whereas no change was observed in the free base homodimers. The changes in the copper(II)–free base dimers are attributed to an enhancement of ISC in the free base half, due to interaction with an unpaired electron in Cu(II) ion of the other half. Estimated ISC rates from the experimental results exhibit a strong correlation with the number of bonds of the linkage but not with the center-to-center distance of the two halves. An expression for the ISC rate in the presence of an unpaired electron is derived. Exchange interaction between the copper unpaired electron and free base π -electrons gives rise to mixing between the excited states of the dimer when the free base moiety is in singlet and triplet excited states, and enhances ISC in the free base part. The observed spacer dependence leads to the suggestion that the ISC rate is governed by through-bond exchange interaction.

1. Introduction

Long-range electronic interaction in molecular ensembles is crucial to understanding intramolecular processes such as electron and energy transfer in biological milieus and artificial molecular systems.^{1–4} Besides the fact that electron and energy transfer occurs through long-range interaction in such systems, natural and artificial large molecular systems often involve a paramagnetic species which is not located in the center of the reaction but may affect photophysical processes through long-range electronic and/or spin–spin interaction.

Among various photophysical processes which might be affected by a remote unpaired electron, one of the simplest processes is intersystem crossing (ISC). Although it is well-known that the ISC rate is governed by spin–orbit (SO) coupling in most molecules,⁵ it is also true that the ISC rate is sometimes much faster than that expected from SO coupling when the system contains a paramagnetic species.^{6,7} To elucidate the role of a “remote” metal unpaired electron in intersystem crossing, we have been investigating porphyrin heterodimers in which only one half has a paramagnetic central metal ion, i.e., copper(II), and the other half is a free base porphyrin. Spacer dependence study of ISC occurring in the diamagnetic moiety of the dimer is expected to lead to a clear understanding of how the remote paramagnetic metal plays a role in terms of ISC rates through long-range interaction.

A great many kinds of porphyrin dimers and oligomers have been studied extensively over the past two decades with relevance to the primary process of photosynthesis and photoharvesting systems.^{4,7–37} Porphyrin dimers with a rigid bridge are advantageous for the systematic investigation of intramolecular processes because the mutual distance and orientation

can be controlled by the spacer units.^{7–13,20–27} Particularly in porphyrin heterodimers having two different metal ions, two moieties are not equivalent due to their different excitation energies and redox potentials. Therefore such features of these porphyrin heterodimers can be utilized not only for designing excellent donor–acceptor systems but also for studying the effects of a remote unpaired electron in one moiety on the other half of the dimer.

Recently, we have shown that efficient intramolecular energy transfer takes place via the triplet manifolds in two rigidly linked copper(II) porphyrin–free base porphyrin dimers, but also that intersystem crossing (ISC) of the free base porphyrin moiety is remarkably enhanced by the copper counterpart by means of fluorescence and transient absorption spectroscopy.⁷ Since the observed ISC rates are different between the two dimers and such effect has not been observed in the corresponding diamagnetic dimers, it is clear that the presence of an unpaired electron in the copper half affects the ISC rate of the free base half. However, a mechanism which accounts for the enhanced ISC by a remote unpaired electron has not been fully substantiated.

In the present work, we investigate spacer dependence of ISC rates of the free base porphyrin moiety in gable-type copper(II)–free base porphyrin heterodimers (Figure 1) involving a new dimer with a phenanthrene bridge. Particularly in the phenanthrene-bridged dimer, the center-to-center distance between the two porphyrins is smaller than those of the other two dimers, i.e., the benzene- and naphthalene-bridged dimers, but the path length to combine the two moieties is the longest among the three. From the fluorescence lifetimes and quantum yields of both series of the free base homodimers and copper(II)–free base heterodimers, we evaluate ISC rates of the free base part in the dimers and show their spacer dependence. Separately, we derive an expression of the ISC rate in the molecular system involving a remote unpaired electron in terms of interaction

* Corresponding author.

† Present address: Radiation Laboratory, University of Notre Dame, Notre Dame, IN 46556.

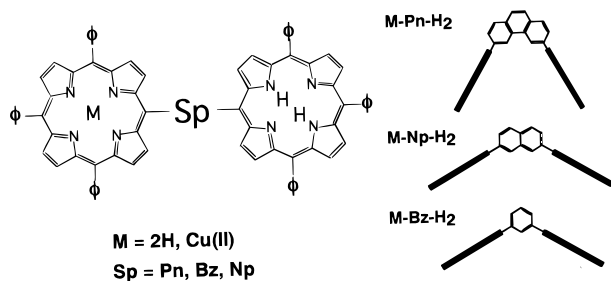


Figure 1. Schematic molecular structures of the copper(II) porphyrin-free base porphyrin dimers bridged via a phenanthrene, a naphthalene, and a benzene.

between the unpaired electron and the π -electrons. On the basis of the derived equation for the ISC rate, we will present a mechanism leading to enhanced ISC through long-range exchange interaction, which is consistent with the observed spacer dependence.

2. Experimental Section

2.1. Measurements. Time-resolved fluorescence measurements were performed on a Hamamatsu C4790 fluorescence lifetime measurement system.⁷ Free base porphyrins were selectively excited at 590 nm by use of a Laser Photonics LN120C Nitro Dye Laser. Emission was dispersed by a Chromex 250IS imaging spectrograph and then detected by a streak scope Hamamatsu C4334 under the single photon counting condition. Both the time- and wavelength-resolved data were transferred to a personal computer through a GPIB interface. Fluorescence lifetimes were determined by fitting the decay profiles produced from the data set summed over an appropriate wavelength window.

Steady-state absorption and emission spectra were taken on a Hitachi 330 spectrophotometer and a Hitachi 850 spectrofluorometer, respectively. For the emission measurements, porphyrins were dissolved in toluene to give a final concentration of $\sim 1 \times 10^{-5}$ M (O.D. at 590 nm = ~ 0.1 with a 10 mm path length). Sample solutions were purged with argon gas and sealed in a quartz cell. Toluene used for solvent was shaken with sulfuric acid following simple distillation, and then neutralized with dilute NaHCO_3 a.q. After washing with water and drying over CaCl_2 , redistillation was carried out on CaH_2 .

2.2. Materials. Porphyrin monomers were prepared and purified according to the reported method.³⁸ The preparation of the benzene- and naphthalene-linked porphyrin dimers was described previously.⁷

Phenanthrene-bridged free base homodimer ($\text{H}_2\text{-Pn-H}_2$) was synthesized essentially in the same method as that of the naphthalene-bridged dimer ($\text{H}_2\text{-Np-H}_2$). The key material for the spacer unit, 3,6-dimethylphenanthrene, was prepared according to the method of Davy et al.³⁹ The dimer was prepared via a stepwise ring closure, and the first condensation of the porphyrin ring was done by the method of Adler et al.⁴⁰ The second ring closure was carried out by the method of Lindsey et al.⁴¹ by using trifluoroacetic acid (TFA) as catalyst. The yield obtained for $\text{H}_2\text{-Pn-H}_2$ with TFA catalysis (25.9%) was higher than that with BF_3 catalysis (12.4%). The free base porphyrin dimer was purified by column chromatography (alumina; CH_2Cl_2 , silica gel; CHCl_3 /hexane) and recrystallization (CHCl_3 /MeOH) repeatedly, to be sufficient for the lifetime measurements.

3,6-Bis[5'-(10',15',20'-triphenylporphyrinyl)]phenanthrene. Anal. Calcd. for $\text{C}_{90}\text{H}_{58}\text{N}_8$ (mol wt 1251.51): C, 86.38; H, 4.67; N, 8.95. Found: C, 86.15; H, 4.96; N, 8.75. FAB-MS,

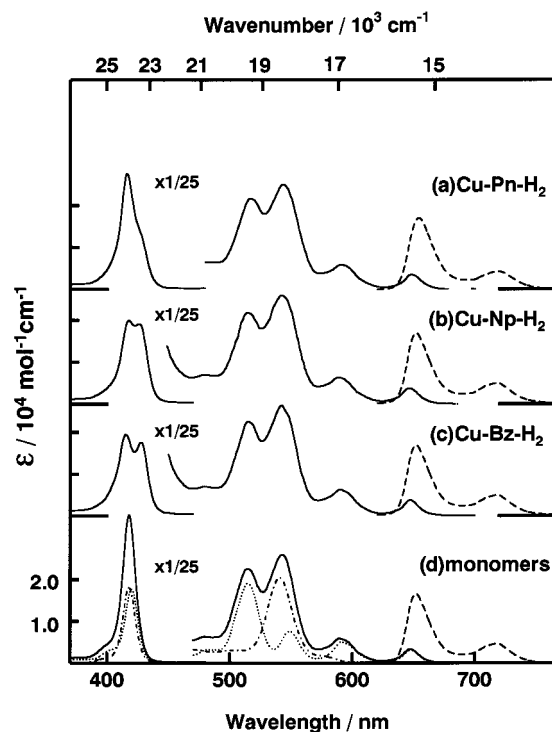


Figure 2. Absorption (—) and emission (---) spectra of (a) Cu-Pn-H₂, (b) Cu-Np-H₂, (c) Cu-Bz-H₂, and (d) a 1:1 linear combination of two monomers, TPPCu and TPPH₂, in toluene at room temperature. In (d), absorption spectra of TPPCu (····) and TPPH₂ (— · —) are also shown. Emission intensities in (a), (b), and (c) are scaled by (a) 10, (b) 13, and (c) 29 times relative to that of (d).

m/z 1251 ($M^+ + 1$). $^1\text{H NMR}(\text{CDCl}_3)$ δ -2.89 (s, 4H), 7.55 (m, 6H), 7.68 (m, 12H), 7.95 (d, $J = 7$ Hz, 4H), 8.09–8.14 (m, 8H), 8.34 (s, 2H), 8.41 (d, $J = 8$ Hz, 2H), 8.56 (d, $J = 8$ Hz, 2H), 8.71–8.73 (m, 12H), 8.85 (d, $J = 5$ Hz, 4H), 9.58 (s, 2H).

Monometalation of $\text{H}_2\text{-Pn-H}_2$ into Cu-Pn-H₂ (Cu-Pn-H₂ denotes [5-[3'-[6'-(10,15,20-triphenyl-21H,23H-porphin-5-yl)]phenanthryl]-10,15,20-triphenyl-porphyrinato]copper(II)- $N^{21},N^{22},N^{23},N^{24}$) was done by reacting with copper(II) acetate, in a manner similar to that for the corresponding benzene- and naphthalene-bridged dimers.⁷ This procedure gives a mixture of bismetall, monometal, and free base porphyrins (i.e., Cu-Pn-Cu, Cu-Pn-H₂, H₂-Pn-H₂). Cu-Pn-H₂ was easily separated from the other two by column chromatography (alumina; CH_2Cl_2 , silica gel; CHCl_3 /hexane) and further purification was carried out on column chromatography and recrystallization (CHCl_3 /MeOH). The final product was identified by FAB-MS spectroscopy; m/z 1313 ($M^+ + 1$). The absorption and emission data are presented under Results.

3. Results

3.1. Absorption Spectra. Figure 2 shows absorption spectra of the three copper(II)-free base porphyrin heterodimers and monomers TPPCu and TPPH₂, along with the 1:1 sum spectrum of the monomers. In all three dimers, the absorption Q-band is almost identical to that of the superposition of the monomers, and thus the interaction between the two moieties should be weak in the Q-band. In contrast, the absorption B-band exhibits an energy splitting depending upon the spacer molecule, while such splitting could not be observed in either the monomers or the sum spectrum.

In the corresponding free base homodimers, similar characteristic features of the absorption Q- and B-bands are observed as shown in Figure 3. The absorption Q-bands of the ho-

TABLE 1: Absorption and Emission Properties of the Monomers and Dimers in Toluene

| | λ_B/nm ($\epsilon/10^5 \text{ mol}^{-1} \text{ cm}^{-1}$) | | λ_Q/nm ($\epsilon/10^3 \text{ mol}^{-1} \text{ cm}^{-1}$) | | | λ_f/nm | | |
|-----------------------------------|--|-----------|--|-----------|-----------|-----------------------|-----|-----|
| TPPH ₂ | 419(4.63) | | 514(19.7) | 549(8.1) | 591(5.5) | 647(3.7) | 652 | 717 |
| TPPCu | 417(4.57) | | 540(20.6) | | | | | |
| H ₂ –Pn–H ₂ | 418(7.26) | 429(sh) | 516(38.9) | 551(18.1) | 592(11.3) | 648(8.0) | 653 | 717 |
| H ₂ –Np–H ₂ | 419(5.43) | 428(5.50) | 516(39.5) | 551(19.4) | 592(11.2) | 648(8.2) | 653 | 717 |
| H ₂ –Bz–H ₂ | 417(4.94) | 428(4.69) | 515(39.8) | 550(18.2) | 592(11.2) | 648(7.9) | 652 | 717 |
| Cu–Pn–H ₂ | 416(6.95) | 428(sh) | 516(22.0) | 543(25.5) | 590(6.3) | 648(3.8) | 653 | 717 |
| Cu–Np–H ₂ | 418(4.98) | 427(4.75) | 515(22.1) | 543(26.1) | 590(6.4) | 648(3.8) | 652 | 717 |
| Cu–Bz–H ₂ | 415(4.86) | 428(4.38) | 515(22.5) | 543(26.4) | 590(6.3) | 648(3.7) | 652 | 717 |

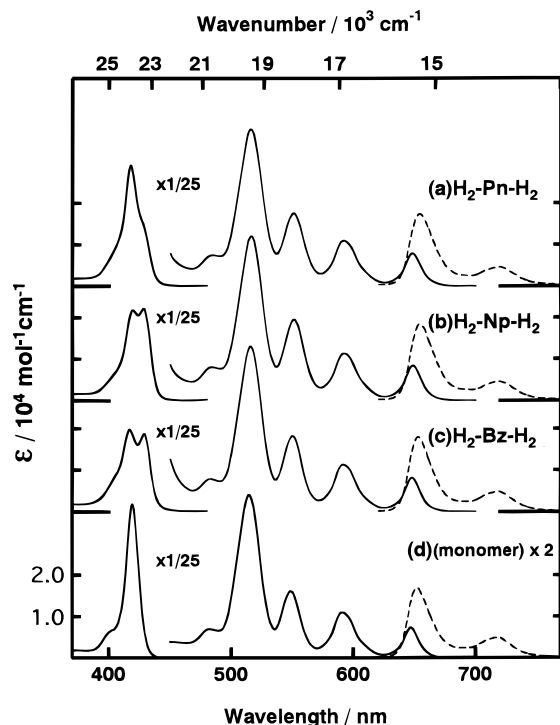


Figure 3. Absorption (—) and emission (---) spectra of (a) H₂–Pn–H₂, (b) H₂–Np–H₂, (c) H₂–Bz–H₂, and (d) the monomer free base TPPH₂ in toluene at room temperature. Note that the intensities in (d) are magnified twice.

modimers are approximately twice as large as that of the free base monomer. It is noted that, in some of reported gable-type free base porphyrin dimers, the absorption Q-bands are red-shifted by 3–5 nm^{25,26} relative to the corresponding monomer. However, such a significant red shift is not observed in the present dimers, and the properties of the absorption Q-band can be described approximately as a superposition of the constituents.⁷ On the other hand, the absorption B-bands of the free base homodimers are not the superposition of those of the monomers but very are similar to the corresponding copper(II)–free base heterodimers. The peak positions of the absorption bands are summarized in Table 1.

It is noted that the lowest excited singlet state of the free base is lower than the corresponding excited state of the copper porphyrin (see Figure 2d). At around 590 nm, copper porphyrin exhibits almost no absorption whereas the free base has appreciable intensity. Thus, we can use this wavelength to excite the free base part in the dimer selectively.

3.2. Fluorescence Spectra, Quantum Yields, and Lifetimes.

The free base monomer exhibits intense fluorescence from the S₁ state, whereas the copper porphyrin does not fluoresce due to rapid intersystem crossing.^{38,42–51} In the copper(II)–free base dimers, fluorescence only from the free base moiety is observed and the spectral shape is the same as that of the monomer independent of the excitation wavelength. Fluorescence spectra

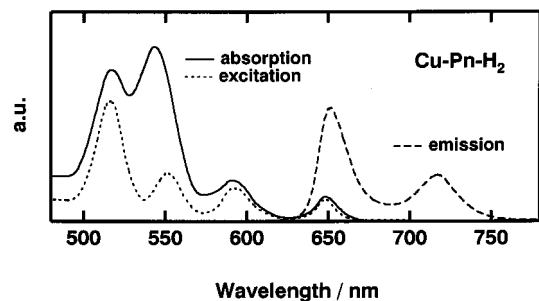


Figure 4. Fluorescence and its excitation spectra of Cu–Pn–H₂ together with the absorption spectrum of the Q-band in toluene.

of the hetero- and homo-dimers are also presented in Figures 2 and 3, respectively. Note that the fluorescence intensities of the copper(II)–free base dimers (Figure 2) are scaled by a factor of 10–30 (see figure caption) relative to the monomer. The fluorescence intensities of the copper(II)–free base dimers are much weaker than the monomer, whereas the free base homodimers do not show any decrease of the fluorescence quantum yield.

Figure 4 compares the fluorescence excitation and absorption spectra of Cu–Pn–H₂. Evidently, the excitation spectrum is coincident with the absorption spectrum of the free base monomer but not with that of the copper(II)–free base dimer (Figures 2 and 3). The other two dimers, Cu–Bz–H₂ and Cu–Np–H₂, also exhibit the same excitation spectrum (not shown). This indicates that energy transfer via porphyrin singlet manifolds does not take place from the copper moiety to the free base in the heterodimers and only the excitation of the free base part yields the free base fluorescence. This situation of copper(II)–free base dimers is quite different from that of zinc(II)–free base dimers which undergo efficient singlet energy transfer.^{8–12, 14,15}

Since the excitation to the copper moiety does not yield S₁ fluorescence of the free base, we compare the relative fluorescence intensity for the selective excitation of the free base moiety. The relative fluorescence intensities of the heterodimers to the monomer are 0.097, 0.080, and 0.035, for Cu–Pn–H₂, Cu–Np–H₂, and Cu–Bz–H₂, respectively. It should be noted that the fluorescence intensity of Cu–Pn–H₂ is the largest while this dimer has the shortest center-to-center distance between the two halves.⁵²

Figure 5 shows transient traces of fluorescence signals of H₂–Pn–H₂ and Cu–Pn–H₂ dimers. In both dimers, fluorescence decays obeying a first-order kinetics. The fluorescence lifetime of Cu–Pn–H₂ was determined as 1.1 ns whereas that of H₂–Pn–H₂ is 12.4 ns. Table 2 presents fluorescence lifetimes and relative fluorescence yields of the copper(II)–free base dimers as well as those of the free base homodimers. Here, the relative fluorescence yield is defined as the fluorescence intensity per the unit concentration of the free base moiety. As listed in Table 2, the variation of the lifetimes is very similar to that of the relative quantum yield: In the heterodimers, fluorescence

TABLE 2: Relative Fluorescence Intensities, Lifetimes, and Evaluated ISC Rates in Toluene

| | I_f | τ_f/ns | $k_{\text{ISC}}/10^7 \text{ s}^{-1}$ | $r_{\text{c-c}}^a/10^{-10} \text{ m}$ | nb^b |
|-----------------------------------|------------------|--------------------|--------------------------------------|---------------------------------------|---------------|
| TPPH ₂ | "1" ^c | 12.5(±0.5) | 6.8(±0.6) | | |
| H ₂ -Pn-H ₂ | 0.96 (±0.05) | 12.4(±0.5) | 7.1(±0.6) | | |
| H ₂ -Np-H ₂ | 1.00 (±0.05) | 12.4(±0.5) | 6.8 (±0.6) | | |
| H ₂ -Bz-H ₂ | 1.02(±0.05) | 12.4(±0.5) | 6.6 (±0.6) | | |
| Cu-Pn-H ₂ | 0.097(±0.01) | 1.1(±0.05) | $0.88(\pm 0.04) \times 10^2$ | 10.9 | 5 |
| Cu-Np-H ₂ | 0.080(±0.01) | 0.89(±0.04) | $1.1(\pm 0.05) \times 10^2$ | 13.2 | 4 |
| Cu-Bz-H ₂ | 0.035(±0.005) | 0.43(±0.04) | $2.3(\pm 0.2) \times 10^2$ | 11.0 | 2 |
| Pd-Bz-H ₂ | 0.85(±0.05) | 10.3(±0.5) | 8.5(±0.8) | | |

^a The center-to-center distance between the two moieties of the dimer, estimated by MM2 calculation.⁵² ^b Number of bonds of the linkage.
^c Fluorescence quantum yield of TPPH₂ is 0.12.^{55,56}

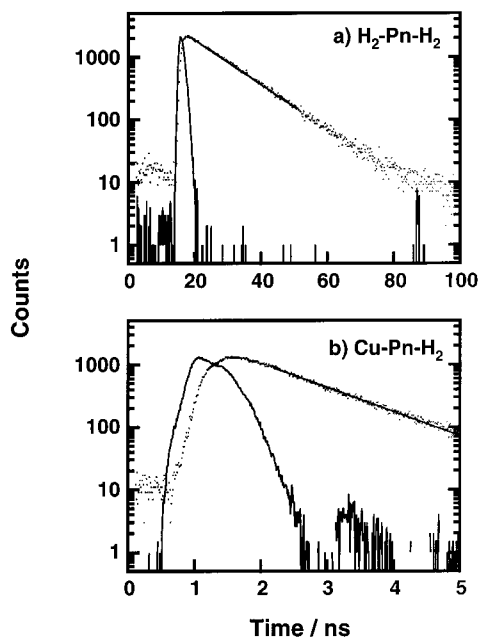


Figure 5. Fluorescence decay profiles of (a) H₂-Pn-H₂ and (b) Cu-Pn-H₂ in toluene at room temperature. Emission data are given by dots, together with the best fitting decay curves. The response for the excitation laser is shown by the solid line.

lifetimes decrease in the same order as that of the relative quantum yield, i.e., Cu-Pn-H₂ > Cu-Np-H₂ > Cu-Bz-H₂, whereas those of the free base homodimers are identical to that of the monomer. Again, the lifetime of the Cu-Pn-H₂ is the longest while the center-to-center distance is the shortest.

For a comparison, the fluorescence quantum yield and lifetime of Pd(II)-Bz-H₂ are also presented in Table 2.

4. Discussion

4.1. Analysis of Fluorescence Yields and Lifetimes. In the phenanthrene-linked copper(II)-free base dimer, Cu-Pn-H₂, the relative fluorescence yield and lifetime of the free base half are remarkably decreased compared to the monomer, as has been observed in Cu-Bz-H₂ and Cu-Np-H₂. It should be noted that the extent of decrease in Cu-Pn-H₂ is smaller than that of the other two copper(II)-free base dimers, despite the fact that the center-to-center distance is the shortest. On the other hand, the quantum yields and lifetimes of the three free base homodimers are essentially the same as those of the monomer. As discussed in ref 7, the decreases in the copper(II)-free base heterodimers can be ascribed to enhanced ISC from the S₁ to T₁ state in the free base moiety but not to other intramolecular processes.

Support for this conclusion came from the transient absorption measurements, which did not show any trace of other intermediates.⁷ In addition, temperature dependence of fluorescence

lifetimes is inconsistent with pathways involving back energy transfer from the free base S₁ to the copper excited states via thermal processes: $\tau(S_1, \text{Cu-Pn-H}_2)$, 1.1 ns at 300 K, 2.3 ns at 77 K; $\tau(S_1, \text{TPPH}_2)$, 12.5 ns at 300 K; 15.5 ns at 77 K. On the basis of the above observations, we conclude that the decreases in fluorescence yields and lifetimes are ascribed to enhancement of ISC in the free base half. In the following, we evaluate ISC rates of the free base moiety and discuss the origin of the spacer dependence.

4.1.1. Estimation of ISC Rates in the Copper(II)-Free Base Dimers. In the dimers, the fluorescence lifetime (τ_f) and yield (ϕ_f) are given by

$$1/\tau_f = k_r + k_{\text{ic}} + k_{\text{isc}} \quad (1)$$

$$\phi_f = k_r / (k_r + k_{\text{ic}} + k_{\text{isc}}) \quad (2)$$

where k_r , k_{ic} , and k_{isc} are the rate constants for radiative decay, internal conversion, and intersystem crossing of the free base moiety, respectively. As has been described in section 3.2, we do not take into account absorption processes of the copper moiety in the dimer. The radiative decay rate constants in the free base moiety can be derived from the ratio of the relative quantum yield to the lifetime by using eqs 1 and 2, and are found to be identical to that of the monomer ($k_r = 9.5 \times 10^6 \text{ s}^{-1}$) within experimental errors. On the other hand, it is difficult to determine the two nonradiative rate constants, k_{ic} and k_{isc} , at the same time from the fluorescence measurements. Here, we assume that the internal conversion rate, k_{ic} , in the dimers is the same as that of the monomer. This is because neither the formation of the dimer nor the insertion of the copper(II) into the other half is expected to affect the internal conversion rate as discussed previously.⁷ In the case of the monomer we can evaluate k_{ic} since the ISC rate in the monomer has been known. In the monomer TPPH₂, the intersystem crossing yield, ϕ_{isc} , was reported as ~ 0.85 (0.82-0.88)^{53,54} whereas the fluorescence quantum yield in toluene was determined as 0.12.^{55,56} By using these values and the monomer lifetime of 12.5 ns, a value of $2.3 \times 10^6 \text{ s}^{-1}$ is obtained for k_{ic} in the monomer.

From the fluorescence lifetime and quantum yields in the dimers, k_{isc} can be estimated by using the values of k_r and k_{ic} and eq 1. Results are summarized in Table 2, along with the center-to-center distance between the two halves and number of bonds on the pathway to link the two porphyrins. The ISC rates in the hybrid dimers are increased by 10–35 times compared to the monomer depending upon the spacer molecule.

4.1.2. Spacer Dependence of the ISC Rates. As has been discussed, it is clear that the presence of the copper(II) ion in the other half affects the ISC rates of the free base half. In addition, this effect is not due to the so-called “heavy atom effect”, since such significant enhancement has not been observed in various zinc(II)-free base dimers.^{8,9b,25} This argument is supported by the fact that Pd-Bz-H₂ shows only a

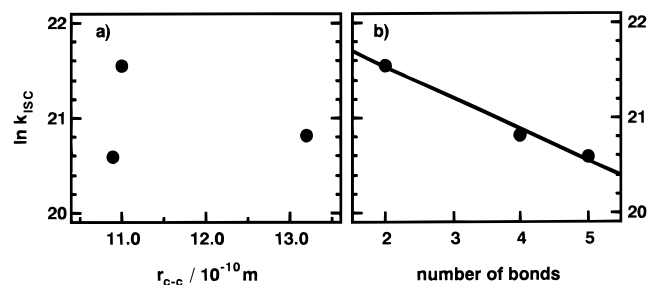


Figure 6. Semilogarithmic plots of k_{isc} versus (a) the center-to-center distance, r_{c-c} , which is calculated on MM2 and (b) number of bonds. The diameter of the circles in the figure indicates the size of experimental errors.

slightly shorter lifetime of the free base moiety (see Table 2) although Pd has a much larger atomic number ($Z = 46$) compared to zinc ($Z = 30$) and copper ($Z = 29$). As proposed previously, the exchange interaction between the π -electrons in the free base half and an unpaired electron in the copper(II) is very likely to gain the ISC rate in the free base moiety. Before discussing the mechanism in detail (see next section), we first consider what property of the dimers determines the spacer dependence of the ISC rates.

Figure 6 shows semilogarithmic plots of k_{isc} (a) vs center-to-center distance of the dimer, r_{c-c} , and (b) vs number of bonds combining the two porphyrins with the shortest pathway. In Figure 6a, there is no clear relation between k_{isc} and r_{c-c} , whereas Figure 6b shows a good linear relation between $\ln k_{isc}$ and number of bonds. This implies that the interaction through the linkage is likely to be dominant in determining the ISC rate rather than the spatial interaction between the two moieties. Figure 6b leads to the suggestion that the ISC rate can be written as

$$k_{isc} \propto \exp \{-\beta(n - 1)\} \quad (3)$$

where $n - 1$ is the number of bonds and β corresponds to the slope of the line in the Figure 6b, which is found to be 0.23 \AA^{-1} .

4.2. Mechanism of Enhanced Intersystem Crossing. In copper(II) porphyrin monomer, exchange interaction between an unpaired electron and porphyrin π -electrons splits porphyrin triplets into so-called “trip-doublets” (2T) and “trip-quartets” (4T) with an energy gap of several hundred cm^{-1} ,^{38,45–49} whereas porphyrin singlet states become “sing-doublet” (2S) states as the whole system.⁴⁵ Nonzero exchange interaction gives rise to mixing between the 2S_1 and 2T_1 states, thus resulting in very fast ISC from the 2S_1 to 2T_1 within a picosecond time scale ($< 8 \text{ ps}$).^{43,44} This value is more than 3 orders of magnitude quicker than that observed in diamagnetic zinc(II) porphyrins ($\sim 2 \text{ ns}$)⁵⁵ wherein ISC rate is governed mainly by SO coupling. Here it is noted that zinc and copper have much the same atomic numbers (30 vs 29).

In the copper(II)–free base dimers, interaction between π -electrons in the free base and an electron in the copper d_{σ} orbital is considered to be much weaker than that in the monomer copper porphyrin. However, such weak interaction is expected to interpret the increase of ISC rates. The aim of this section is to derive an expression for the ISC rate in terms of the interaction between the copper half and the free base half and present a mechanism which is consistent with the observed spacer dependence.

4.2.1. Wave Functions of the Excited States of the Free Base Half in Copper(II)–Free Base Porphyrin Dimers. In the present

section, we derive wave functions of the excited states of the copper(II) porphyrin–free base porphyrin dimers where the free base part is excited and the copper half is in the ground state. Here we only consider excitations in the free base π -system but do not involve (π, π^*) excitations in the copper moiety, since we can conclude that the ISC does not compete against any other intramolecular process and is independent of (π, π^*) transitions in the copper half.

In free base monomer and typical diamagnetic metalloporphyrins, the characteristic nature of the two lowest excited singlet and triplet states can be well explained by four transitions between two HOMOs and two LUMOs in the porphyrin π -system.^{57,58} In the free base monomer with D_{2h} symmetry, two HOMOs are b_{1u} and a_u orbital, whereas two LUMOs are b_{2g} and b_{3g} .^{42,59} When the dimer system has an unpaired d-electron in the other half, the system can be described as linear combinations of the products of the d-orbital and free base π -orbitals. This is analogous to the treatment of the copper porphyrin monomer^{38,45} although the copper d-electron in our case is located rather away from the free base π -electron system. The ground state of the system consisting of the four free base π -orbitals and a copper d-orbital is doublet, and the wave functions for $S_z = 1/2$ and $-1/2$ substates are given by

$$\begin{aligned} |G\alpha\rangle &= |d_{a_u} \overline{a_u} b_{1u} \overline{b_{1u}}| \\ |G\beta\rangle &= |\overline{d_{a_u}} \overline{a_u} b_{1u} \overline{b_{1u}}| \end{aligned} \quad (4)$$

where d stands for the copper unpaired electron and the overbar ($\overline{\quad}$) stands for β spin.

In monomer porphyrin π -system, the two lowest excited singlet states, i.e., Q and B states, are approximately described as a 1:1 mixture of two configurations due to the characteristic nature of the porphyrin π -system.^{42,55} For the excited states of the dimer where the free base half is in the excited singlet states and the copper(II) is the ground state, the following four configurations can be given as the $S_z = 1/2$ states:

$$\begin{aligned} |Q_x\alpha\rangle &= \{|d \cdot^1(b_{1u} b_{2g})\rangle - |d \cdot^1(a_u b_{3g})\rangle\} / \sqrt{2} \\ |Q_y\alpha\rangle &= \{|d \cdot^1(b_{1u} b_{3g})\rangle + |d \cdot^1(a_u b_{2g})\rangle\} / \sqrt{2} \\ |B_x\alpha\rangle &= \{|d \cdot^1(b_{1u} b_{2g})\rangle + |d \cdot^1(a_u b_{3g})\rangle\} / \sqrt{2} \\ |B_y\alpha\rangle &= \{|d \cdot^1(b_{1u} b_{3g})\rangle - |d \cdot^1(a_u b_{2g})\rangle\} / \sqrt{2} \end{aligned} \quad (5)$$

where

$$\begin{aligned} |d \cdot^1(b_{1u} b_{2g})\rangle &= \{|d_{a_u} \overline{a_u} b_{1u} \overline{b_{2g}}\rangle - |d_{a_u} \overline{a_u} b_{1u} b_{2g}\rangle\} / \sqrt{2} \\ |d \cdot^1(a_u b_{3g})\rangle &= \{|d_{a_u} \overline{b_{3g}} b_{1u} \overline{b_{1u}}\rangle - |d_{a_u} \overline{b_{3g}} b_{1u} b_{1u}\rangle\} / \sqrt{2} \\ |d \cdot^1(b_{1u} b_{3g})\rangle &= \{|d_{a_u} \overline{a_u} b_{1u} \overline{b_{3g}}\rangle - |d_{a_u} \overline{a_u} b_{1u} b_{3g}\rangle\} / \sqrt{2} \\ |d \cdot^1(a_u b_{2g})\rangle &= \{|d_{a_u} \overline{b_{2g}} b_{1u} \overline{b_{1u}}\rangle - |d_{a_u} \overline{b_{2g}} b_{1u} b_{1u}\rangle\} / \sqrt{2} \end{aligned} \quad (6)$$

The two states $|Q_x\alpha\rangle$ and $|Q_y\alpha\rangle$ correspond to the first excited singlet states of the free base monomer, Q_x and Q_y states, respectively, and they have almost equal energy and transition moment but different symmetry. Similarly, $|B_x\alpha\rangle$ and $|B_y\alpha\rangle$ correspond to the second singlet excited states. For the symmetrical reason, $|Q_x\alpha\rangle$ can mix with $|B_x\alpha\rangle$ but not with $|Q_y\alpha\rangle$ and $|B_y\alpha\rangle$. Since the wave functions with y -symmetry (B_{2u} representation) compose essentially the same energy matrix as that of x -symmetry (B_{3u} representation), hereafter we will show

only x -symmetry wave functions and matrix elements. The corresponding $S_z = -1/2$ states for x -symmetry are

$$\begin{aligned} |Q_x\beta\rangle &= \{|\bar{d}\cdot^1(b_{1u}b_{2g})\rangle - |\bar{d}\cdot^1(a_u b_{3g})\rangle\}/\sqrt{2} \\ |B_x\beta\rangle &= \{|\bar{d}\cdot^1(b_{1u}b_{2g})\rangle + |\bar{d}\cdot^1(a_u b_{3g})\rangle\}/\sqrt{2} \end{aligned} \quad (7)$$

In contrast to the (monomer) porphyrin singlet states, the two lowest triplet states can be described rather as a single configuration.^{38,42} When the free base moiety is in a triplet, the whole system of the dimer is a coupled triplet–doublet system and S_z numbers are $3/2$, $1/2$, $-1/2$, and $-3/2$. Thus, in the dimer, the wave functions for $S_z = 3/2$ substates of the dimer can be written as

$$\begin{aligned} S_z = 3/2 \\ |T_{ax}(+1)\alpha\rangle &= |d\cdot^3(a_u b_{3g})_{+1}\rangle = |da_u b_{3g} \bar{b}_{1u} \bar{b}_{1u}\rangle \\ |T_{bx}(+1)\alpha\rangle &= |d\cdot^3(b_{1u} b_{2g})_{+1}\rangle = |da_u \bar{a}_u \bar{b}_{1u} b_{2g}\rangle \end{aligned} \quad (8)$$

where T_a and T_b stand for two electronic excited triplet states, i.e., (T_1 , T_2) states of the free base moiety and $(+1)$ stands for the spin-quantum number of the triplet state. Whether T_a or T_b is the lower depends on the peripheral substituents of the macrocycle.^{42,38,55} Here, we assume that the lowest electronic excited state is T_b , i.e., the state with $^3(b_{1u}b_{2g})$ configuration, since the corresponding monomer has $^3(b_{1u}b_{2g})$ configuration as the lowest.^{42,55}

The wave functions for $S_z = -3/2$, $1/2$, and $-1/2$ substates of T_{bx} state are

$$S_z = -3/2 \\ |T_{bx}(-1)\beta\rangle = |\bar{d}\cdot^3(b_{1u} b_{2g})_{-1}\rangle = |\bar{d}a_u \bar{a}_u \bar{b}_{1u} \bar{b}_{2g}\rangle \quad (9)$$

$$\begin{aligned} S_z = 1/2 \\ |T_{bx}(+1)\beta\rangle &= |\bar{d}\cdot^3(b_{1u} b_{2g})_{+1}\rangle = |\bar{d}a_u \bar{a}_u \bar{b}_{1u} \bar{b}_{2g}\rangle \\ |T_{bx}(0)\alpha\rangle &= |d\cdot^3(b_{1u} b_{2g})_0\rangle = \{|\bar{d}a_u \bar{a}_u \bar{b}_{1u} \bar{b}_{2g}\rangle + \\ &\quad |\bar{d}a_u \bar{a}_u \bar{b}_{1u} b_{2g}\rangle\}/\sqrt{2} \end{aligned} \quad (10)$$

$$\begin{aligned} S_z = -1/2 \\ |T_{bx}(0)\beta\rangle &= |\bar{d}\cdot^3(b_{1u} b_{2g})_0\rangle = \{|\bar{d}a_u \bar{a}_u \bar{b}_{1u} \bar{b}_{2g}\rangle + \\ &\quad |\bar{d}a_u \bar{a}_u \bar{b}_{1u} b_{2g}\rangle\}/\sqrt{2} \\ |T_{bx}(-1)\alpha\rangle &= |d\cdot^3(b_{1u} b_{2g})_{-1}\rangle = |\bar{d}a_u \bar{a}_u \bar{b}_{1u} \bar{b}_{2g}\rangle \end{aligned} \quad (11)$$

If the exchange coupling between the free base triplet and the copper doublet electrons is strong, the wave functions in the coupled triplet–doublet system would mix with each other to a large extent and then split into quartet and doublet states. However, if the coupling is weak, mixing is small and wave functions in eqs 8–11 will remain as a good basis set.³⁴ In the next section we will consider matrix elements of this triplet–doublet system and derive an expression for the ISC rate.

4.2.2. Matrix Elements Leading to Enhanced ISC in the Copper(II)–Free Base Porphyrin Dimer. According to the well-known theory of radiationless transitions,⁶¹ transition probability per unit time is given by

$$w_{fi} = \frac{4\pi^2}{h} |\langle \psi_f | V | \psi_i \rangle|^2 \rho \quad (12)$$

where V is a perturbation term of the Hamiltonian responsible for the transition from the initial state ψ_i to the final state ψ_f , ρ is the density of the final states, and h is Planck's constant.

Since the initial states of ISC are ψ_{Q_i} states, e.g., $|Q_x\alpha\rangle$, and the final states are ψ_{T_j} states, e.g., $|T_{bx}(+1)\beta\rangle$ and $|T_{bx}(0)\alpha\rangle$, the ISC rate of the free base moiety is written as

$$k_{isc} \propto \sum_i \sum_j |\langle \psi_{T_j} | V | \psi_{Q_i} \rangle|^2 \rho_j \quad (13)$$

Nonzero exchange interaction between the π -electrons in the free base and a copper unpaired electron gives rise to the coupling matrix elements between ψ_{Q_i} and ψ_{T_j} states. For example, the $|Q_x\alpha\rangle$ state has coupling with $|T_{bx}(+1)\beta\rangle$ and $|T_{bx}(0)\alpha\rangle$ while the $|Q_x\beta\rangle$ state has coupling with $|T_{bx}(0)\beta\rangle$ and $|T_{bx}(-1)\alpha\rangle$. The coupling matrix elements which lead to the ISC transitions are given by

$$\begin{aligned} \langle Q_x\alpha | V | T_{bx}(0)\alpha \rangle &= -\langle Q_x\beta | V | T_{bx}(0)\beta \rangle = \\ &\quad -\frac{1}{2\sqrt{2}} (K_{b_{1u}} - K_{b_{2g}}) \\ \langle Q_x\alpha | V | T_{bx}(+1)\beta \rangle &= -\langle Q_x\beta | V | T_{bx}(-1)\alpha \rangle = \\ &\quad \frac{1}{2} (K_{b_{1u}} - K_{b_{2g}}) \end{aligned} \quad (14)$$

where $K_{b_{1u}}$ and $K_{b_{2g}}$ are the exchange interaction between the copper unpaired electron and free base π -electron in b_{1u} and b_{2g} orbitals, respectively.

$$\begin{aligned} K_{b_{1u}} &= (b_{1u} d | d b_{1u}) \\ K_{b_{2g}} &= (b_{2g} d | d b_{2g}) \end{aligned} \quad (15)$$

The whole energy matrix is presented in Table 3. Substituting eq 13 into eq 14, we obtain the following expression for the ISC rate:

$$k_{isc} \propto c^2 (K_{b_{1u}} - K_{b_{2g}})^2 \quad (16)$$

As a result, the ISC rate is proportional to the square of a difference of the two exchange integrals between the unpaired electron in the copper(II) and π -electrons in the free base HOMO and LUMO.

4.2.3. Spacer Dependence of Exchange Interaction. As has been discussed in section 4.1.2, the spacer dependence of the ISC rates shows a good correlation with the number of bonds combining the two moieties but not with the center-to-center distance of the dimer. According to the mechanism above, the ISC rate is given as a function of the exchange integrals between the electrons in the free base π -system and a copper d orbital. Therefore, the sizes of exchange integrals are expected to depend on the number of bonds of the spacer. Such an interaction may be called a through-bond interaction,^{61–63} in analogy to what has been found in long-range intramolecular electron and energy transfer processes.^{64–66} Here, we further consider the ISC rate in eq 16 in terms of the spacer dependence.

Based on the through-bond model originally presented by McConnell,⁶¹ exchange coupling between the two terminal moieties which are linked with n pieces of bridges can be given in a modified form⁶²

$$K_i = C_i \left(\frac{t}{\Delta_i} \right)^{(n-1)} \quad (17)$$

where Δ_i is an energy difference between a virtual orbital of the bridge and a porphyrin π -orbital i , and t is the coupling term between the bridged orbitals. C_i is a function including Δ_i , the coupling term between the edge of the bridge and the

TABLE 3: Energy Matrices of Excited States in a System Porphyrin Singlet/Triplet Coupled with Cooper Doublet (x-symmetry)

| $S_z = 3/2$ | | | | | |
|----------------------------------|----------------------------------|------------------------------------|--|------------------------------------|-------------------------------------|
| $ T_{ax}(+1)\alpha\rangle$ | | | $ T_{bx}(+1)\alpha\rangle$ | | |
| $J_1 - K_1 - (K_{au} + K_{b3g})$ | | | 0 $J_2 - K_2 - (K_{b1u} + K_{b2g})$ | | |
| $S_z = 1/2$ | | | | | |
| $ B_x\alpha\rangle$ | $ Q_x\alpha\rangle$ | $ T_{ax}(+1)\beta\rangle$ | $ T_{bx}(+1)\beta\rangle$ | $ T_{ax}(0)\alpha\rangle$ | $ T_{bx}(0)\alpha\rangle$ |
| $J - K + 2K' + 2K'' - (A + B)/2$ | δ_ϵ | $(K_{au} - K_{b3g})/2$ | $(K_{b1u} - K_{b2g})/2$ | $-(K_{au} - K_{b3g})/2\sqrt{2}$ | $-(K_{b1u} - K_{b2g})/2\sqrt{2}$ |
| | $J - K + 2K' - 2K'' - (A + B)/2$ | $-(K_{au} - K_{b3g})/2$ | $(K_{b1u} - K_{b2g})/2$ | $(K_{au} - K_{b3g})/2\sqrt{2}$ | $-(K_{b1u} - K_{b2g})/2\sqrt{2}$ |
| | | $J_1 - K_1$ | 0 | $-(K_{au} + K_{b3g})/\sqrt{2}$ | 0 |
| | | | $J_2 - K_2$ | 0 | $-(K_{b1u} + K_{b2g})/\sqrt{2}$ |
| | | | | $J_1 - K_1 - (K_{au} + K_{b3g})/2$ | 0 |
| | | | | | $J_2 - K_2 - (K_{b1u} + K_{b2g})/2$ |
| $S_z = -1/2$ | | | | | |
| $ B_x\beta\rangle$ | $ Q_x\beta\rangle$ | $ T_{ax}(0)\beta\rangle$ | $ T_{bx}(0)\beta\rangle$ | $ T_{ax}(-1)\alpha\rangle$ | $ T_{bx}(-1)\alpha\rangle$ |
| $J - K + 2K' + 2K'' - (A + B)/2$ | δ_ϵ | $(K_{au} - K_{b3g})/2\sqrt{2}$ | $(K_{b1u} - K_{b2g})/2\sqrt{2}$ | $-(K_{au} - K_{b3g})/2$ | $-(K_{b1u} - K_{b2g})/2$ |
| | $J - K + 2K' - 2K'' - (A + B)/2$ | $-(K_{au} - K_{b3g})/2\sqrt{2}$ | $(K_{b1u} - K_{b2g})/2\sqrt{2}$ | $(K_{au} - K_{b3g})/2$ | $-(K_{b1u} - K_{b2g})/2$ |
| | | $J_1 - K_1 - (K_{au} + K_{b3g})/2$ | 0 | $-(K_{au} + K_{b3g})/\sqrt{2}$ | 0 |
| | | | $J_2 - K_2 - (K_{b1u} + K_{b2g})/2$ | 0 | $-(K_{b1u} + K_{b2g})/\sqrt{2}$ |
| | | | | $J_1 - K_1$ | 0 |
| | | | | | $J_2 - K_2$ |
| $S_z = -3/2$ | | | | | |
| $ T_{ax}(-1)\beta\rangle$ | | | $ T_{bx}(-1)\beta\rangle$ | | |
| $J_1 - K_1 - (K_{au} + K_{b3g})$ | | | 0 $J_2 - K_2 - (K_{b1u} + K_{b2g})$ | | |

In these matrices

$$J_1 = 2\{(b_{1u}b_{1u}|a_u a_u) + (b_{1u}b_{1u}|b_{3g}b_{3g}) + (b_{1u}b_{1u}|dd)\} + (b_{1u}b_{1u}|b_{1u}b_{1u}) + (a_u a_u|b_{3g}b_{3g}) + (a_u a_u|dd) + (b_{3g}b_{3g}|dd)$$

$$J_2 = 2\{(b_{1u}b_{1u}|a_u a_u) + (a_u a_u|b_{2g}b_{2g}) + (a_u a_u|dd)\} + (a_u a_u|a_u a_u) + (b_{1u}b_{1u}|b_{2g}b_{2g}) + (b_{1u}b_{1u}|dd) + (b_{2g}b_{2g}|dd)$$

$$J = (J_1 + J_2)/2$$

$$K_{b1u} = (b_{1u}d|db_{1u}), K_{b2g} = (b_{2g}d|db_{2g}), K_{au} = (a_u d|da_u), K_{b3g} = (b_{3g}d|db_{3g})$$

$$K_1 = (b_{1u}a_u|a_u b_{1u}) + (b_{1u}b_{3g}|b_{3g}b_{1u}) + (a_u b_{3g}|b_{3g}a_u) + K_{b1u}$$

$$K_2 = (b_{1u}a_u|a_u b_{1u}) + (a_u b_{2g}|b_{2g}a_u) + (b_{1u}b_{2g}|b_{2g}b_{1u}) + K_{au}$$

$$K = (K_1 + K_2)/2$$

$$K' = \{(a_u b_{3g}|b_{3g}a_u) + (b_{1u}b_{2g}|b_{2g}b_{1u})\}/2$$

$$K'' = (a_u b_{3g}|b_{2g}b_{1u})$$

$$A = (K_{au} + K_{b1u})/2$$

$$B = (K_{b3g} + K_{b2g})/2$$

$$\delta_\epsilon = (J_1 - J_2) - (K_1 - K_2) + 2\{(a_u b_{3g}|b_{3g}a_u) - (b_{1u}b_{2g}|b_{2g}b_{1u})\} + \{K_{au} - K_{b1u} + K_{b3g} - K_{b2g}\}/2$$

where

$$(ab|cd) = \int \phi_a^*(1) \phi_c^*(2) e^2/r_{12} \phi_b(1) \phi_d(2) dr_1 dr_2$$

porphyrin π -orbital i , and exchange interaction between d_σ and π -electrons in the copper porphyrin. Therefore the ISC rate in eq 16 is rewritten as

$$k_{isc} = c' \left[C_{b1u} \left(\frac{t}{\Delta_{b1u}} \right)^{(n-1)} - C_{b2g} \left(\frac{t}{\Delta_{b2g}} \right)^{(n-1)} \right]^2 \quad (18)$$

Since the energy of the virtual bridge orbital is expected to be much higher than the energies of the porphyrin LUMOs and HOMOs, we can assume $\Delta_{b1u} \approx \Delta_{b2g} \approx \Delta$. Thus the ISC rate is given by

$$k_{isc} = c' (C_{b1u} - C_{b2g})^2 \left(\frac{t}{\Delta} \right)^{2(n-1)} \quad (19)$$

Accordingly we obtain the expression

$$k_{isc} = C \exp\{-\beta(n-1)\} \quad (20)$$

where

$$\beta = -2 \ln(t/\Delta) \quad (21)$$

In the above, β depends on the interaction between the bridge orbitals and the energy difference between the porphyrin orbital and the virtual bridge orbital. It is noted that β does not depend on the interaction between the copper electron and porphyrin π -electrons. From Figure 6b, we have obtained $\beta = 0.23 \text{ \AA}^{-1}$, which agrees with values observed for electron and energy transfer in similar series of aromatically bridged porphyrin dimers.^{10a} This agreement supports the contention that the through-bond exchange interaction plays a dominant role in determining the ISC rate.

4.2.4. Other Factors. Although the ISC rates show an exponential dependence on the number of bonds, we might have to consider effects of π -electrons in the arene spacers. Recently, it was reported that the spacer arene mediates singlet–singlet

energy transfer in a series of zinc(II) porphyrin–free base porphyrin dimers bridged by a benzene, a naphthalene, and an anthracene.⁹ In this series of head-to-tail type dimers, not only the distance but also the number of bonds between the donor and acceptor is the same. The observed energy transfer rates in the benzene- and naphthalene-bridged dimers are much the same but that for the anthracene-bridged dimer is approximately twice as large as the other two. They suggested mediation of energy transfer by the bridging chromophore, possibly through (π, π^*) excited states of the aromatic spacer.

In our case, the lowest singlet excitation energies of benzene, naphthalene, and phenanthrene are 38 400, 32 200, and 28 900 cm^{-1} , respectively.⁶⁷ Since phenanthrene has the lowest energy among the three, the largest influence by (π, π^*) excited states of the spacer would be expected in the phenanthrene-linked dimer. However, the observed ISC rate is the slowest in this dimer and the semilogarithmic plot of ISC rates in Figure 6b shows a quite good linear relation. This implies that the effect from the (π, π^*) excited states of the spacer molecule is not so large as that which could be observed appreciably. This situation is similar to what was reported in a series of the polyene-bridged dimers by Osuka et al.^{10b} In their dimers, the energy transfer rate decreases exponentially with an increase of the length of the polyene bridge, despite the fact that the energy of the lowest excited state of the spacer shifts lower in response to the length of the polyene.

5. Conclusions

The observed spacer dependence not only leads to the conclusion that the through-bond interaction is likely to be dominant rather than that of through-space in governing the ISC rate, but also provides support for the contention that exchange interaction between a metal unpaired electron in one half and π -electrons in the other half enhances ISC in the free base half. These results show that a remote unpaired electron in the metal ion can play an important role in relaxation processes of the localized part in supramolecular systems through long-range interaction.

Acknowledgment. The authors are grateful to Professors K. Eguchi and K. Kakinuma for the measurements of FAB MASS and 500 MHz ^1H NMR spectra and thank Professor Emeritus K. Yamamoto for the use of his photoreaction apparatus in Tokyo Institute of Technology. This work was partially supported by a Grant-in-Aid for Scientific Research from the Ministry of Education, Science, Culture and Sports Japan (No. 11740318, 11694061).

Supporting Information Available: ^1H NMR data for the compounds obtained in the synthetic procedures of $\text{H}_2\text{-Pn-H}_2$ and $\text{H}_2\text{-Np-H}_2$. This information is available free of charge via the Internet at <http://pubs.acs.org>.

References and Notes

- (1) (a) van Grondelle, R.; Dehher, J. P.; Gillbro, T.; Sundstrom, V. *Biochim. Biophys. Acta* **1994**, *1187*, 1. (b) Huber, R. *Angew. Chem., Int. Ed. Engl.* **1989**, *28*, 848.
- (2) Sauvage, J.-P.; Collin, J.-P.; Chambron, J.-C.; Guillerez, S.; Balzani, V.; Barigelli, F.; De Cola, L.; Flamigni, L. *Chem. Rev.* **1994**, *94*, 993.
- (3) Speiser, S. *Chem. Rev.* **1996**, *96*, 1953.
- (4) (a) Ward, M. R. *Chem. Soc. Rev.* **1997**, *26*, 365. (b) Kurreck, H.; Huber, M. *Angew. Chem., Int. Ed. Engl.* **1995**, *34*, 849. (c) Wasielewski, M. R. *Chem. Rev.* **1992**, *92*, 435. (d) Sessler, J. L. *Isr. J. Chem.* **1992**, *32*, 449. (e) Gust, D.; Moore, T. A. *Adv. Photochem.* **1991**, *16*, 1.
- (5) Turro, N. J. In *Moeden Molecular Photochemistry*; University Science Books: California, 1991; Chapter 6.
- (6) Kalyanasundram, K. In *Photochemistry of Polypyridine and Porphyrin Complexes*; Academic Press: London, 1992; Chapters 1 and 2 and references therein.
- (7) Asano-Someda, M.; Kaizu, Y. *Inorg. Chem.* **1999**, *38*, 2303.
- (8) (a) Hsiao, J.-S.; Krueger, B. P.; Wagner, R. W.; Johnson, T. E.; Delaney, J. K.; Mauzerall, D. C.; Fleming, G. R.; Lindsey, J. S.; Bocian, D. F.; Donohoe, R. J. *J. Am. Chem. Soc.* **1996**, *118*, 11181. (b) Strachan, J.-P.; Gentemann, S.; Seth, J.; Kalsbeck, W. A.; Linsey, J. S.; Holten, D.; Bocian, D. F. *J. Am. Chem. Soc.* **1997**, *119*, 11191. (c) Strachan, J.-P.; Gentemann, S.; Seth, J.; Kalsbeck, W. A.; Linsey, J. S.; Holten, D.; Bocian, D. F. *Inorg. Chem.* **1998**, *37*, 1191. (d) Yang, S. I.; Seth, J.; Balasubramanian, T.; Kim, D.; Lindsey, J. S.; Holten, D.; Bocian, D. F. *J. Am. Chem. Soc.* **1999**, *121*, 4008.
- (9) (a) Jensen, K. K.; van Berlekom, S. B.; Kajanus, J.; Mårtensson, J.; Albinsson, B. *J. Phys. Chem. A* **1997**, *101*, 2218. (b) Kilså, K.; Kajanus, J.; Mårtensson, J.; Albinsson, B. *J. Phys. Chem. B* **1999**, *103*, 7329.
- (10) (a) Osuka, A.; Maruyama, K.; Yamazaki, I.; Tamai, N. *Chem. Phys. Lett.* **1990**, *165*, 392. (b) Osuka, A.; Tanabe, N.; Kawabata, S.; Yamazaki, I.; Nishimura, Y. *J. Org. Chem.* **1995**, *60*, 7177. (c) Kawabata, S.; Yamazaki, I.; Nishimura, Y.; Osuka, A. *J. Chem. Soc., Perkin Trans. 2* **1997**, *101*, 479.
- (11) Sessler, J. L.; Wang, B.; Harriman, A. *J. Am. Chem. Soc.* **1995**, *117*, 704.
- (12) (a) Rodriguez, J.; Kirmaier, C.; Johnson, M. R.; Friesner, R. A.; Holten, D.; Sessler, J. L. *J. Am. Chem. Soc.* **1991**, *113*, 1652. (b) Sessler, J. L.; Capuano, V. L.; Harriman, A. *J. Am. Chem. Soc.* **1993**, *115*, 4618.
- (13) (a) de Rege, P. J. F.; Williams, S. A.; Therien, M. J. *Science* **1995**, *269*, 1409. (b) de Rege, P. J. F.; Therien, M. J. *Inorg. Chim. Acta* **1996**, *242*, 211.
- (14) (a) Brookfield, R. L.; Ellul, H.; Harriman, A.; Porter, G. J. *Chem. Soc., Faraday Trans. 2* **1986**, *82*, 219. (b) Anton, J. A.; Loach, P. A.; Govindjee. *Photochem. Photobiol.* **1978**, *28*, 235.
- (15) (a) Regev, A.; Galili, T.; Levanon, H.; Harriman, A. *Chem. Phys. Lett.* **1986**, *131*, 140. (b) Gonen, O.; Levanon, H. *J. Chem. Phys.* **1986**, *84*, 4132.
- (16) (a) Mialocq, J. C.; Giannotti, C.; Maillard, P.; Momenteau, M. *Chem. Phys. Lett.* **1984**, *112*, 87. (b) Schwarz, F. P.; Gouterman, M.; Muljiani, Z.; Dolphin, D. H. *Bioinorg. Chem.* **1972**, *2*, 1.
- (17) Selensky, R.; Holten, D.; Windsor, M. W.; Paine, J. B., III; Dolphin, D.; Gouterman, M.; Thomas, J. C. *Chem. Phys.* **1981**, *60*, 33.
- (18) Kaizu, Y.; Maekawa, H.; Kobayashi, H. *J. Phys. Chem.* **1986**, *90*, 4234.
- (19) Ohno, O.; Ogasawara, Y.; Asano, M.; Kajii, Y.; Kaizu, Y.; Obi, K.; Kobayashi, H. *J. Phys. Chem.* **1987**, *91*, 4269.
- (20) (a) Sessler, J. L.; Hugdahl, J.; Johnson, M. R. *J. Org. Chem.* **1986**, *51*, 2838. (b) Sessler, J. L.; Johnson, M. R.; Lin, T.-Y.; Creager, S. E. *J. Am. Chem. Soc.* **1988**, *110*, 3659.
- (21) (a) Osuka, A.; Maruyama, K. *J. Am. Chem. Soc.* **1988**, *110*, 4454. (b) Osuka, A.; Maruyama, K.; Yamazaki, I.; Tamai, N. *J. Chem. Soc., Chem. Commun.* **1988**, 1243.
- (22) Chang, C. K.; Abdalmuhdi, I. *J. Org. Chem.* **1983**, *48*, 5388.
- (23) (a) Helms, A.; Heiler, D.; McLendon, G. *J. Am. Chem. Soc.* **1991**, *113*, 4325. (b) Helms, A.; Heiler, D.; McLendon, G. *J. Am. Chem. Soc.* **1992**, *114*, 6227.
- (24) Wagner, R. W.; Johnson, T. E.; Li, F.; Lindsey, J. S. *J. Org. Chem.* **1995**, *60*, 5266.
- (25) Sessler, J. L.; Johnson, M. R.; Lin, T.-Y. *Tetrahedron* **1989**, *45*, 4767.
- (26) Osuka, A.; Liu, B.; Maruyama, K. *J. Org. Chem.* **1993**, *58*, 3582.
- (27) Osuka, A.; Maruyama, K.; Mataga, N.; Asahi, T.; Yamazaki, I.; Tamai, N. *J. Am. Chem. Soc.* **1990**, *112*, 4958.
- (28) (a) Gust, D.; Moore, T. A.; Moore, A. L.; Gao, F.; Luttrull, D.; DeGraziano, J. M.; Ma, X. C.; Makings, L. R.; Lee, S.-J.; Trier, T. T.; Bittersmann, E.; Seely, G. R.; Woodward, S.; Bensasson, R. V.; Rougée, M.; De Schryver, F. C.; Van der Auweraer, M. *J. Am. Chem. Soc.* **1991**, *113*, 3638. (b) Gust, D.; Moore, T. A.; Moore, A. L.; Leggett, L.; Lin, S.; DeGraziano, J. M.; Hermant, R. M.; Nicodem, D.; Craig, P.; Seely, G. R.; Nieman, R. A. *J. Phys. Chem.* **1993**, *97*, 7926. (c) DeGraziano, J. M.; Liddell, P. A.; Leggett, L.; Moore, A. L.; Moore, T. A.; Gust, D. *J. Phys. Chem.* **1994**, *98*, 1758.
- (29) Gust, D.; Moore, T. A.; Moore, A. L.; Devadoss, C.; Liddell, P. A.; Hermant, R.; Nieman, R. A.; Demanche, L. J.; DeGraziano, J. M.; Gouni, I. *J. Am. Chem. Soc.* **1992**, *114*, 3590.
- (30) (a) Tamiaki, H.; Nomura, K.; Maruyama, K. *Bull. Chem. Soc. Jpn.* **1993**, *66*, 3062. (b) Tamiaki, H.; Nomura, K.; Maruyama, K. *Bull. Chem. Soc. Jpn.* **1994**, *67*, 1863.
- (31) (a) Harriman, A.; Heitz, V.; Ebersole, M.; van Willigen, H. *J. Phys. Chem.* **1994**, *98*, 4982. (b) Chambron, J.-C.; Harriman, A.; Heitz, V.; Sauvage, J.-P. *J. Am. Chem. Soc.* **1993**, *115*, 6109.
- (32) (a) Harriman, A.; Odeobel, F.; Sauvage, J.-P. *J. Am. Chem. Soc.* **1995**, *117*, 7, 9461. (b) Flamigni, L.; Barigelli, F.; Armaroli, N.; Ventura, B.; Collin, J.-P.; Sauvage, J.-P.; Williams, J. A. G. *Inorg. Chem.* **1999**, *38*, 661.

- (33) Asano-Someda, M.; Ichino, T.; Kaizu, Y. *J. Phys. Chem. A* **1997**, *101*, 4484.
- (34) Asano-Someda, M.; van der Est, A.; Krueger, U.; Stehlik, D.; Kaizu, Y.; Levanon, H. *J. Phys. Chem. A* **1999**, *103*, 6704.
- (35) Kadish, K. M.; Guo, N.; Van Caemelbecke, E.; Froiio, A.; Paolesse, R.; Monti, D.; Traliatesta, P.; Boschi, T.; Prodi, L.; Bolletta, F.; Zaccaroni, N. *Inorg. Chem.* **1998**, *37*, 2358.
- (36) Hungerford, G.; van der Auweraer, M.; Chambron, J.-C.; Heitz, V.; Sauvage, J.-P.; Pierre, J.-L.; Zurita, D. *Chem. Eur. J.* **1999**, *5*, 2089.
- (37) Tsuchiya, S. *J. Am. Chem. Soc.* **1999**, *121*, 48.
- (38) Asano, M.; Kaizu, Y.; Kobayashi, H. *J. Chem. Phys.* **1988**, *89*, 6567.
- (39) (a) Davy, J. R.; Jessup, P. J.; Reiss, J. A. *J. Chem. Educ.* **1975**, *52*, 747. (b) Moradpour, A.; Kagan, H.; Baes, M.; Morren, G.; Martin, R. H. *Tetrahedron* **1975**, *31*, 2139. (c) Buquet, A.; Couture, A.; Lablache-Combiere, A. *J. Org. Chem.* **1979**, *44*, 2300.
- (40) (a) Alder, A. D.; Longo, F. R.; Finarell, J. D.; Goldmacher, J.; Assour, J.; Korsakoff, L. *J. Org. Chem.* **1967**, *32*, 476. (b) Tabushi, I.; Kugimiya, S.; Kinnaird, M. G.; Sasaki, T. *J. Am. Chem. Soc.* **1985**, *107*, 4192. (c) Tabushi, I.; Sasaki, T. *Tetrahedron Lett.* **1982**, *23*, 1913.
- (41) (a) Lindsey, J. S.; Hsu, H. C.; Schreiman, I. C. *Tetrahedron Lett.* **1986**, *27*, 4969. (b) Lindsey, J. S.; Schreiman, I. C.; Hsu, H. C.; Kearney, P. C.; Marguerettaz, A. M. *J. Org. Chem.* **1987**, *52*, 827.
- (42) Gouterman, M. In *The Porphyrins*; Dolphin, D., Ed.; Academic Press: New York, 1978; Vol. 3, p 1.
- (43) Kobayashi, T.; Huppert, D.; Straub, K. D.; Renzepis, P. M. *J. Chem. Phys.* **1979**, *70*, 1720.
- (44) Rodriguez, J.; Kirmaier, C.; Holten, D. *J. Am. Chem. Soc.* **1989**, *111*, 6500.
- (45) Ake, R. L.; Gouterman, M. *Theor. Chim. Acta* **1969**, *15*, 20.
- (46) (a) Gouterman, M.; Mathies, R. A.; Smith, B. E.; Caughey, W. S. *J. Chem. Phys.* **1970**, *52*, 3795. (b) Eastwood, D.; Gouterman, M. *J. Mol. Spectrosc.* **1969**, *30*, 437.
- (47) Canters, G. W.; van der Waals, J. H. In *The Porphyrins*; Dolphin, D., Ed.; Academic Press: New York, 1978; Vol. 3, p 531.
- (48) (a) van Dorp, W. G.; Canters, G. W.; van der Waals, J. H. *Chem. Phys. Lett.* **1975**, *35*, 450. (b) Noort, M.; Jansen, G.; Canters, G. W.; van der Waals, J. H. *Spectrochim. Acta* **1976**, *32*, 1371. (c) van Dijk, N.; van der Waals, J. H. *Mol. Phys.* **1979**, *38*, 1211. (d) van der Poel, W. A. J.; Nuijs, A. M.; van der Waals, J. H. *J. Phys. Chem.* **1986**, *90*, 1537.
- (49) (a) Kim, D.; Holten, D.; Gouterman, M. *J. Am. Chem. Soc.* **1984**, *106*, 2793. (b) Yan, X.; Holten, D. *J. Phys. Chem.* **1988**, *92*, 5982.
- (50) Asano-Someda, M.; Kaizu, Y. *J. Photochem. Photobiol. A* **1995**, *87*, 23.
- (51) (a) Liu, F.; Cunningham, K. L.; Uphues, W.; Fink, G. W.; Schmolt, J.; McMillin, D. R. *Inorg. Chem.* **1995**, *34*, 2015. (b) Cunningham, K. L.; McNett, K. M.; Pierce, R. A.; Davis, K. A.; Harris, H. H.; Flack, D. M.; McMillin, D. R. *Inorg. Chem.* **1997**, *36*, 608.
- (52) Molecular modeling calculation was carried out by molecular mechanics MM2, performed by CS chem 3D Pro software (Cambridge Soft Corp.)
- (53) (a) Harriman, A. *J. Chem. Soc., Faraday Trans. 1* **1980**, *76*, 1978. (b) Harriman, A.; Porter, G.; Wilowska, A. *J. Chem. Soc., Faraday Trans. 2* **1983**, *79*, 807.
- (54) Lee, W. A.; Grätzel, M.; Kalyanasundram, K. *Chem. Phys. Lett.* **1984**, *107*, 308.
- (55) Ohno, O.; Kaizu, Y.; Kobayashi, H. *J. Chem. Phys.* **1985**, *82*, 1779.
- (56) The S₁ fluorescence quantum yield of TPPZn (in benzene), $\phi = 0.033$, is used as the standard.
- (57) Gouterman, M. *J. Chem. Phys.* **1959**, *30*, 1139.
- (58) Kobayashi, H. *J. Chem. Phys.* **1959**, *30*, 1362.
- (59) Sekino, H.; Kobayashi, H. *J. Chem. Phys.* **1981**, *75*, 3477.
- (60) Bixon, M.; Jortner, J. *J. Chem. Phys.* **1968**, *48*, 715.
- (61) McConnell, H. M. *J. Chem. Phys.* **1961**, *35*, 508.
- (62) Newton, M. D. *Chem. Rev.* **1991**, *91*, 767.
- (63) (a) Paddon-Row, M. N. *Acc. Chem. Res.* **1994**, *27*, 18. (b) Paddon-Row, M. N. *Acc. Chem. Res.* **1982**, *15*, 245.
- (64) (a) Closs, G. L.; Piotrowiak, P.; MacInnis, J. M.; Fleming, G. R. *J. Am. Chem. Soc.* **1988**, *110*, 2652. (b) Closs, G. L.; Johnson, M. D.; Miller, J. R.; Piotrowiak, P. *J. Am. Chem. Soc.* **1989**, *111*, 3751.
- (65) Oevering, H.; Verhoeven, J. W.; Paddon-Row, M. N.; Cotsaris, E.; Hush, N. S. *Chem. Phys. Lett.* **1988**, *143*, 488.
- (66) Sigman, M. E.; Closs, G. L. *J. Phys. Chem.* **1991**, *95*, 5012.
- (67) Murov, S. L. In *Hand Book of Photochemistry*, 2nd ed., revised and expanded; Murov, S. L., Carmichael, I., Hug, G. L., Eds.; Marcel Dekker: New York, 1993; Section 1.